Computational Analysis of Bio-Inspired Corrugated Airfoil with Varying Corrugation Angle

Khan MA*, Padhy C, Nandish M and Rita K

Department of Aerospace Engineering, Gitam University, Hyderabad, India

Abstract

A computational study is conducted to investigate the aerodynamic performance of a newly designed corrugated airfoil of dragonfly at range of low Reynolds number 15000-38000. This study represents the transient nature of corrugated airfoils at low Reynolds number where flow is assumed to be laminar, unsteady, incompressible and two dimensional. This research comprises of the investigation of the aerodynamic performance of various corrugation configurations at different corrugated angle (i.e., 4°, 8°, 12°) with varying pitch length and peak height along the span wise and chordwise directions. The 12° corrugated angle is incorporated in the new modified design with varying pitch length, corrugated angle and peak height to achieve the higher lift to drag ratio. The simulation is carried out using Ansys CFD as a simulation tool and ICEM CFD as a modeling tool for 2-D corrugated airfoil. The design features of corrugated airfoil used in this research is not used in earlier studies. The simulation includes a sharp interface cartesian grid-based meshing and k-ε model for turbulence model. The computational results show that the newly designed corrugated aero foil generates more lift and less drag compared to flat plate and NACA 0015 aero foil and also helps in preventing large scale flow separation.

Keywords: 2-D corrugated aero foil; Dragonfly; Low Reynolds number; Ansys CFX/Fluent; Flat plate; NACA 0015

Introduction

Among natural flyers, dragonflies have unique features and flight capabilities. Their flight performance far exceeds many other flying insect species. The complex morphology of the dragonfly wing cross section (airfoil) is very different from the traditional closed, thick and smooth airfoils of low Reynolds number airplane. Okama et al. [1] isolated the influence of different geometrical parameters and showed that the surface texture or the roughness of wings results in an increased maximum lift coefficient, C_{Lmax} and increases maximum lift to drag ratio $(L/D)_{max}$. Dragonfly wings are highly corrugated, which increases the stiffness and strength of the wing significantly and results in a lightweight structure with good aerodynamic performance. Corrugation provokes an early transition to turbulent flow over the two-dimensional airfoil, permitting reattachment of the flow over the wing called laminar bubble.

Dragonfly being a natural flyer the vein and the membrane structure are flexible in nature as shown in Figure 1 Therefore; it will be difficult to predict the behavior of corrugated wing during flight condition. It has a flapping frequency between 30 Hz and 50 Hz. Flapping flights of dragonflies has been extensively studied by Savage et al., Alexander [2], Wakeling and Ellington. According to Rees [3] the fluid flowing over the airfoil gets trapped in the corrugation valleys where it either becomes stagnant or rotates slowly, resulting in virtual profiling over the corrugated airfoil.

Kesel [4] noticed trapped vortices present in the folds that serve to change the effective profile of the airfoil. With the advent of bio-inspired aerial vehicle, it has become clear that there is much that can be learnt from insect flight that could be translated into engineered systems. At a higher Reynolds number, it is hypothesized that the dragonfly actually flies without wing flapping [5]. The negative pressure developed in these corrugations contributes to the excessive lift. It is the reason that makes further investigation into the aerodynamic aspect of dragonfly wing worthwhile. This study focuses on the aerodynamic characteristics of the newly modified corrugated design and the flow pattern around a dragonfly corrugated wing of a particular cross-section (Figure 1).

Figure 1: (a) & (b) Dragonfly corrugated wing vein structure.

Materials and Methods

Geometry selection and design

Three types of the airfoils are used in the present study i.e., triangular wave modeling at different corrugation angles (i.e., 4°, 8° and 12°) and varying pitch length, Modified wing 1(MW-1) and Modified wing 2(MW-2). The dragonfly airfoil used in the present study is cambered

*Corresponding author: Khan MA, Gitam University, Department of Aerospace Engineering, Hyderabad, India, Tel: +91-891 2790 101; E-mail: Khan.akhtar24@gmail.com

and has the chord length of 110 mm, peak height 2 mm and thickness of wing is 2 mm [6-9].

Computational domain: After modeling the wings in CATIA, it is exported to ANSYS 15(FLUENT) and the analysis of the aerodynamic performance of corrugated aerofoil is carried out by using structured grid Navier-stokes equation. Grid points are denser near the airfoil wall region to capture flow characteristics accurately [7,8].

$$\frac{\partial u_i}{\partial t} + \frac{\partial}{\partial X_j}(u_i u_j) = -\frac{1}{\rho}\frac{\partial p}{\partial X_i} + v\frac{\partial^2}{\partial X_j^2}(u_i)$$

Boundary conditions

The flow around the corrugated airfoil is assumed to be laminar, incompressible, unsteady and 2-dimensional. The outlet of the domain was set to pressure outlet where the value of the gauge pressure is set to zero (Table 1).

Results and Discussion

From the analysis, we observed that as the corrugation angle

Dynamic viscosity (μ)	1.7895×10^{-5} Ns/m
Density	1.23 Kg/m^3
Inflow velocity (U$_\infty$)	2.067 m/s
Reynolds number	15000

Table 1: Boundary conditions.

Figure 2: (a) 2-D view of 4° corrugation angle at α =0°; (b) 2-D view of 8° corrugation angle at α =0°;(c) 3-D view of 8 degree corrugation angle at α =0°; (d) 2-D view of 12° corrugation angle at α =0°

Figure 3: (a) Computational domain of non-uniform cartesian grid; (b) Enlarged view of grid refinement.
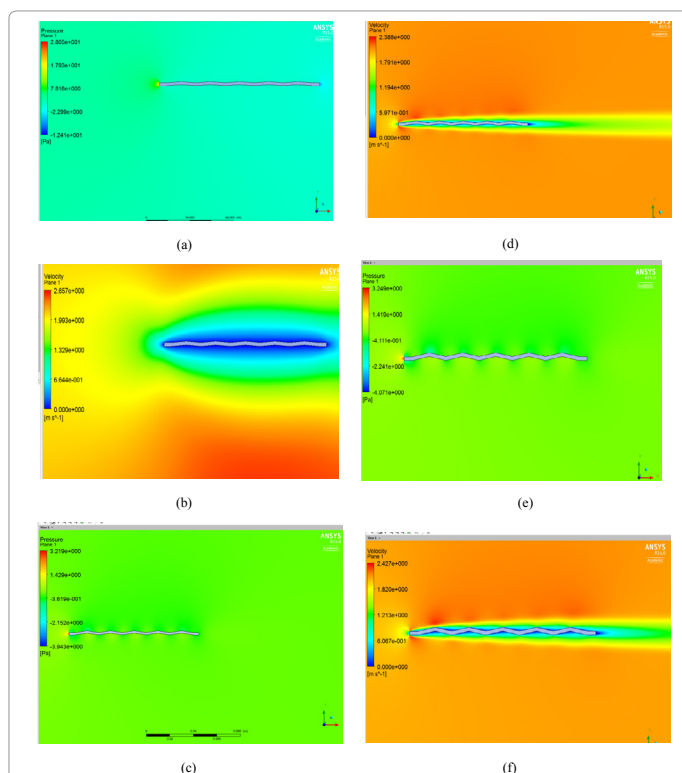
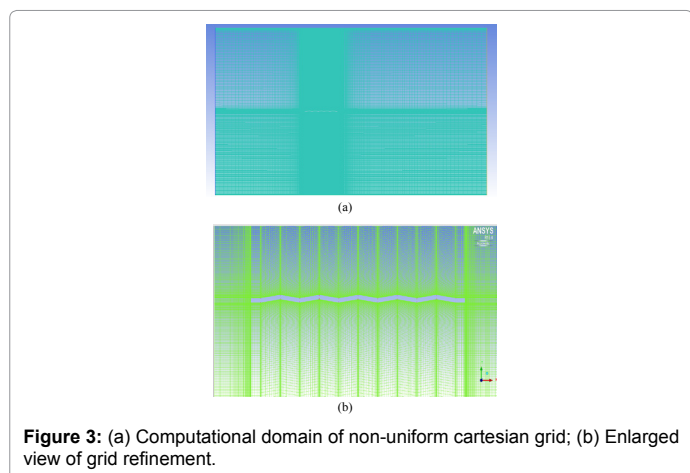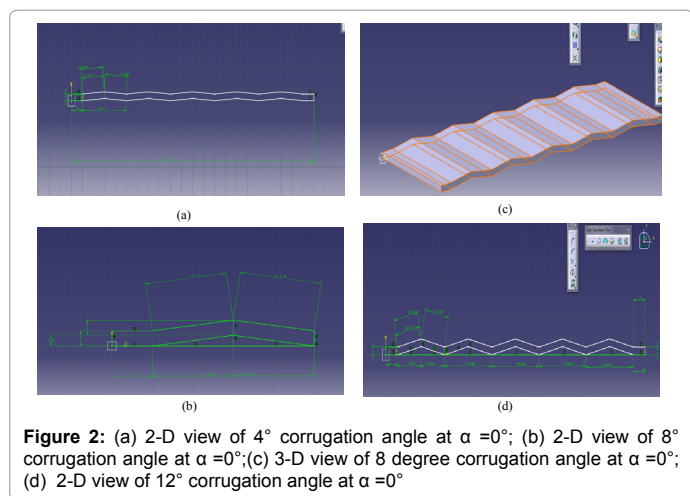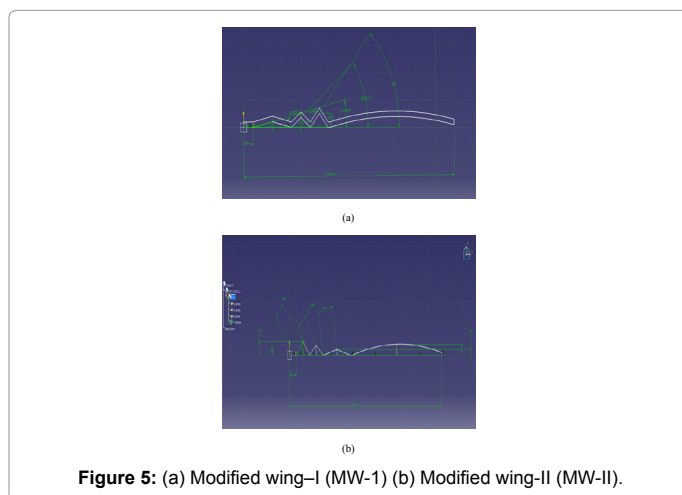**Figure 4:** The instantaneous flow field at α= 0° (a) pressure plot for 4° corrugation angle (b) velocity plot for 4°corrugation angle (c) pressure plot for 8° corrugation angle (d) velocity plot for 8° corrugation angle (e) pressure plot for 12° corrugation angle (f) velocity plot for 12° corrugation angle.

Figure 5: (a) Modified wing–I (MW-1) (b) Modified wing-II (MW-II).

increases, the flow separation delays and the also the velocity increases which gives a better lift to drag ratio than the lower corrugation angles. Out of these 12° corrugation angle performed much better giving high L/D ratio compared to others (Figures 2-5).

Based on this analysis, 12° corrugation angle is incorporated in the new design with increasing angles of corrugation with a curved profile near the trailing edge region which helps in delaying the flow separation and also reduces vortices, hence reducing drag (Tables 2 and 3).

Design and analysis of modified wing

Now taking above design in consideration the corrugated design

is modified with increasing corrugation angles in ascending and descending order (i.e., 12°, 36° and 48°) and vice versa with increasing peak heights and having a curved profile at the trailing edge as shown in Figures 5(a) and 5(b).

### Analysis of modified wing-I (MW-I) and analysis of modified wing-II (MW-II)

In this it is clearly observed that as the highest corrugation angle is at the beginning of the wing, the flow is getting separated at the first peak itself and flow is reattaching at the end of the wing (Figures 6-8).

| Type of wings	Angle of attack(degree)	$\frac{L}{D}$ Ratio
4° Corrugation angle	0°	0.7731
8° Corrugation angle	0°	1.468
12° Corrugation angle	0°	1.9

Table 2: Variation of L/D ratio for different corrugation.

| Type of wings	Angle of attack	C_L	C_D	$\frac{L}{D}$ Ratio
MW-I	0°	3.0987	0.95442	3.25
MW-II	0°	3.108	1.14878	3.108
Flat plate	0°	~ 0	~ 0	$3.12 \times 10^{-6} \sim 0$
NACA 0015	0°	0.016065	0.55803	0.028

Table 3: Result comparison.
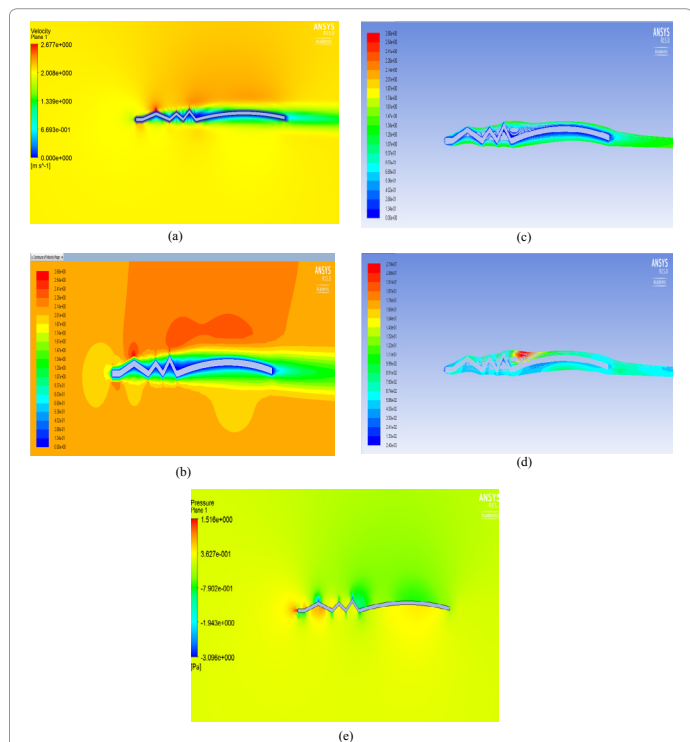
Figure 6: The instantaneous flow field at α = 0° for MW-I (a) Velocity distribution (b) Velocity contour (c) Velocity pathline (d) Turbulence contour (e) Pressure distribution As we can observe, the velocity is high at the peaks of the corrugations and at the valleys the velocity is zero indicating reversed flow or vortices formation as shown in Figure 6 (a). The flow velocity is trapped into the valleys of modified wing-I as shown in Figure 6 (c) which helps in delaying separation and flow will stick to the surface. The pressure distribution shows high pressure at the stagnation points and lowest pressure at peaks and at the valleys there is low pressure indicating reversed flow as shown in Figure 6 (e). Analysis of modified wing-II (MW-II).
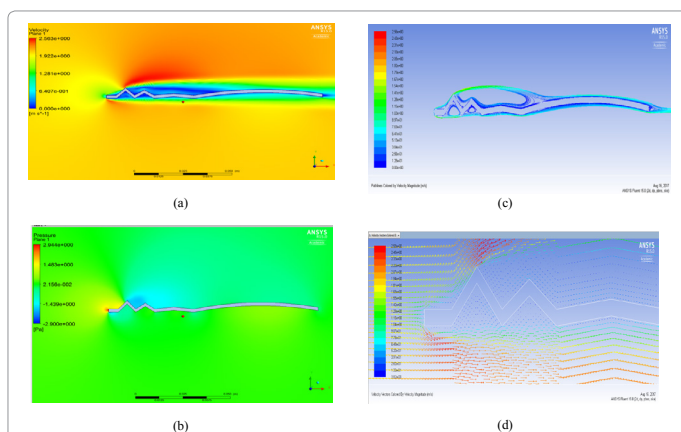
Figure 7: The instantaneous flow field at α = 0° for MW-I (a) Velocity distribution (b) pressure distribution (c) Velocity pathline d) Velocity vector. Comparisons of modified corrugated wings with flat plate and NACA 0015.
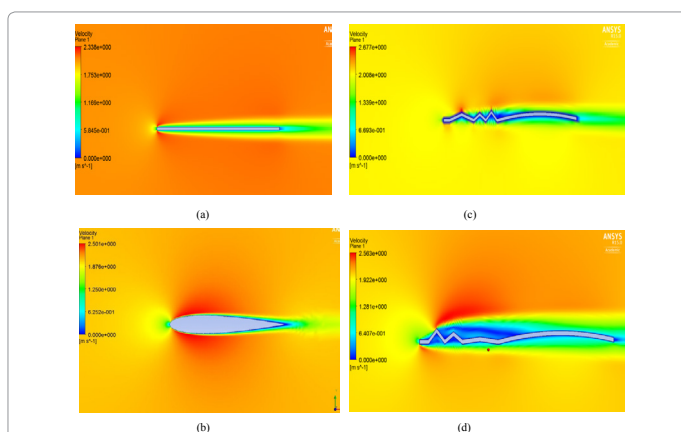
Figure 8: The flow field at angle of attack, α = 0° (a) velocity distribution of flat plate (b) velocity distribution of NACA 0015 (c) velocity distribution for MW-I (D) velocity distribution for MW-II.

Comparisons of modified corrugated wings with flat plate and NACA 0015

The comparative observations made through Figures 8 (a) to 8(d), have been represented in Table 3.

Summary and Conclusion

A computational simulation on dragonfly corrugated wing cross section is performed at Reynolds numbers between 15000 and 38000. The results of the corrugated airfoils are compared with flat plate and NACA 0015 airfoil. We observed that the vortices formed on the corrugated aerofoil and shed into its wakes produces lower integral force fluctuation because of the its upstream peak height which allows the flow to reattach near the trailing edge of the airfoil by delaying flow separation [10-12]. The aerodynamic performance i.e., (L/D) ratio of the modified wing –I (MW-I) is better compared to MW-II and NACA 0015 at 0° angle of attack. It is found that the design criteria being used, and simulation carried out on MW-I and MW-II is giving much better result as compared to that of earlier studies. For MW-I as the angle of attack increases L/D ratio increases as the flow remains attached to the surface and get trapped into the valley, hence the performance of our design is much better than compared to earlier studies being conducted on the aerodynamic behavior of the corrugated dragonfly airfoil.

References

1. Okamoto M, Yasuda K, Azuma A (1996) Aerodynamic characteristics of the wings and the body of a dragonfly. J experimental biology 199: 281-294.

2. Alexander D (1984) Unusual phase relationships between the forewing and hindwing in flying dragonflies. J Experimental Biology 109: 379-383.

3. Rees CJC (1975) Form and function in corrugated insect wings. Nature 256: 200-203.

4. Kesel AB, Philippi U, Nachtigall W (1998) Biomechanical aspects of insect wings- an analysis using the finite element method. Computers in Biology and Medicine 28: 423-437.

5. Chen YH, Skote M (2015) Study of lift enhancing mechanisms via comparison of two distinct flapping patterns in the dragonfly sympetrum flaveolum. Physics of Fluids 27: 033604.

6. David-Elie L, Seifert A (2009) Simplified dragonfly airfoil aerodynamics at Reynolds numbers below 8000. Physics of fluids: 071901.

7. Ho WH, New TH, Matare E (2017) Unsteady CFD analysis of an oscillating aerofoil inspired by dragonfly wings. Topical problems of fluid mechanics.

8. Lazos BS (2005) Biologically inspired fixed-wing configuration studies. J Aircraft 42: 5.

9. Steven L, Brunton, Rowley CW (2010) Unsteady aerodynamic models for agile flight at low reynolds number. AIAA Aerospace Science.

10. Wakeling JM, Ellington CP (1997) Dragonfly flight I. gliding flight and steady-state aerodynamic forces. J Experimental Biology 200: 543-556.

11. Sudhakar Y, Vengadesan S (2009) Flight force production by flapping insect wings in inclined stroke plane kinematics Computers and Fluids: 1-13.

12. Levy D, Seifert A (2010) Parameter study of simplified dragonfly airfoil geometry at Reynolds number of 6000. J Theor Biol 266: 691-702.